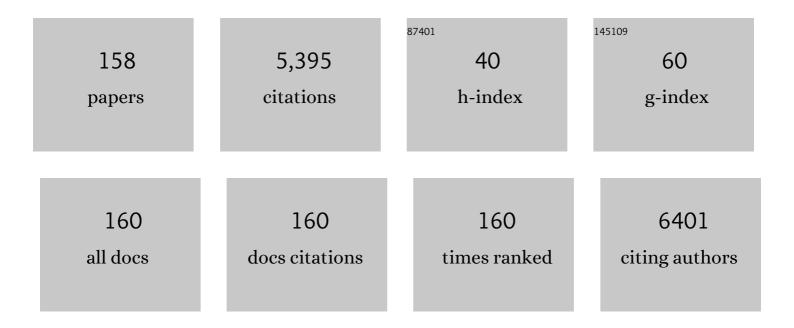
Jeong Gil Seo

List of Publications by Year in descending order

Source: https://exaly.com/author-pdf/3911797/publications.pdf Version: 2024-02-01



#	Article	IF	CITATIONS
1	Synergistically Interfaced Bifunctional Transition Metal Selenides for Highâ€Rate Hydrogen Production Via Urea Electrolysis. ChemCatChem, 2022, 14, .	1.8	6
2	Highly porous, hierarchical peanut-like Ecandrewsite binary metal oxide nanostructures for the high-efficiency detoxification of organic dyes from wastewater. Ceramics International, 2022, 48, 1057-1067.	2.3	3
3	Enhanced Hydrogenation of Levulinic Acid over Ordered Mesoporous Alumina‣upported Catalysts: Elucidating the Effect of Fabrication Strategy. ChemSusChem, 2022, 15, .	3.6	7
4	Yolk-shell nickel–cobalt phosphides as bifunctional catalysts in the solvent-free hydrogenation of Levulinic acid to gamma-Valerolactone. Renewable Energy, 2022, 191, 763-774.	4.3	9
5	Cu ₂ O/CuO Electrocatalyst for Electrochemical Reduction of Carbon Dioxide to Methanol. Electroanalysis, 2021, 33, 705-712.	1.5	34
6	Growth of binder free mesoporous 3D-CuCo2O4 electrocatalysts with high activity and stability for electro-oxidation of methanol. Ceramics International, 2021, 47, 3322-3328.	2.3	11
7	Highly porous honeycombâ€like activated carbon derived using cellulose pulp for symmetric supercapacitors. International Journal of Energy Research, 2021, 45, 4385-4395.	2.2	13
8	Application of 2-methylfuran and 5-methylfurfural for the synthesis of C16 fuel precursor over fibrous silica-supported heteropoly acid-functionalized ionic liquid. Korean Journal of Chemical Engineering, 2021, 38, 1170-1178.	1.2	4
9	Interplay between electrochemical reactions and mechanical responses in silicon–graphite anodes and its impact on degradation. Nature Communications, 2021, 12, 2714.	5.8	51
10	Constructive designing of ternary metal oxide as an anode material for high performance lithiumâ€ion batteries. International Journal of Energy Research, 2021, 45, 16592-16602.	2.2	7
11	Characterisation of bacterial nanocellulose and nanostructured carbon produced from crude glycerol by Komagataeibacter sucrofermentans. Bioresource Technology, 2021, 342, 125918.	4.8	16
12	Catalytic C-C coupling of furanic platform chemicals to high carbon fuel precursors over supported ionic liquids. Applied Catalysis A: General, 2021, 628, 118421.	2.2	6
13	Triboelectrification-based particulate matter capture utilizing electrospun ethyl cellulose and PTFE spheres. Atmospheric Environment: X, 2021, 12, 100138.	0.8	6
14	Low-temperature selective dehydrogenation of methylcyclohexane by surface protonics over Pt/anatase-TiO2 catalyst. International Journal of Hydrogen Energy, 2020, 45, 738-743.	3.8	43
15	Covalently decorated crown ethers on magnetic graphene oxides as bi-functional adsorbents with tailorable ion recognition properties for selective metal ion capture in water. Chemical Engineering Journal, 2020, 389, 123421.	6.6	50
16	Hierarchically assembled porous TiO2 nanoparticles with enhanced photocatalytic activity towards Rhodamine-B degradation. Colloids and Surfaces A: Physicochemical and Engineering Aspects, 2020, 586, 124199.	2.3	16
17	An advanced and highly efficient Ce assisted NiFe-LDH electrocatalyst for overall water splitting. Sustainable Energy and Fuels, 2020, 4, 312-323.	2.5	125
18	Mechanically reinforced-CNT cathode for Li-O2 battery with enhanced specific energy via ex situ pore formation. Chemical Engineering Journal, 2020, 385, 123841.	6.6	19

#	Article	IF	CITATIONS
19	Encapsulation of Phase-Changing Eutectic Salts in Magnesium Oxide Fibers for High-Temperature Carbon Dioxide Capture: Beyond the Capacity–Stability Tradeoff. ACS Applied Materials & Interfaces, 2020, 12, 518-526.	4.0	13
20	MgO insertion endowed strong basicity in mesoporous alumina framework and improved CO2 sorption capacity. Journal of CO2 Utilization, 2020, 42, 101294.	3.3	12
21	Support effects on catalysis of low temperature methane steam reforming. RSC Advances, 2020, 10, 26418-26424.	1.7	14
22	Substrate Effect of Platinum-Decorated Carbon on Enhanced Hydrogen Oxidation in PEMFC. ACS Omega, 2020, 5, 26902-26907.	1.6	10
23	Supported Bimetallic Catalysts for the Solvent-Free Hydrogenation of Levulinic Acid to γ-Valerolactone: Effect of Metal Combination (Ni-Cu, Ni-Co, Cu-Co). Catalysts, 2020, 10, 1354.	1.6	15
24	Hierarchical novel <scp> NiCo ₂ O ₄ </scp> / <scp> BiVO ₄ </scp> hybrid heterostructure as an advanced anode material for rechargeable lithium ion battery. International Journal of Energy Research, 2020, 44, 12126-12135.	2.2	8
25	Effects of metal cation doping in CeO ₂ support on catalytic methane steam reforming at low temperature in an electric field. RSC Advances, 2020, 10, 14487-14492.	1.7	20
26	Key factor for the anti-Arrhenius low-temperature heterogeneous catalysis induced by H ⁺ migration: H ⁺ coverage over support. Chemical Communications, 2020, 56, 3365-3368.	2.2	27
27	Unveiling the carbonation mechanism in molten salt-promoted MgO-Al2O3 sorbents. Journal of CO2 Utilization, 2020, 39, 101153.	3.3	9
28	Interface modulation of a layer-by-layer electrodeposited FexCo(1â^'x)P/NiP@CC heterostructure for high-performance oxygen evolution reaction. Sustainable Energy and Fuels, 2020, 4, 1863-1874.	2.5	22
29	Hydroxyalkylation/alkylation of 2-methylfuran and furfural over niobic acid catalysts for the synthesis of high carbon transport fuel precursors. Sustainable Energy and Fuels, 2020, 4, 3018-3028.	2.5	18
30	Eutectic mixture promoted CO2 sorption on MgO-TiO2 composite at elevated temperature. Journal of Environmental Sciences, 2019, 76, 80-88.	3.2	19
31	Solvothermal Synthesis of Mesoporous 3D uCo ₂ O ₄ Hollow Tubes as Efficient Electrocatalysts for Methanol Electroâ€Oxidation. ChemCatChem, 2019, 11, 6078-6085.	1.8	9
32	Dehydrogenation of Ethane via the Mars–van Krevelen Mechanism over La _{0.8} Ba _{0.2} MnO _{3â°î´} Perovskites under Anaerobic Conditions. Journal of Physical Chemistry C, 2019, 123, 26272-26281.	1.5	14
33	Governing factors of supports of ammonia synthesis in an electric field found using density functional theory. Journal of Chemical Physics, 2019, 151, 064708.	1.2	13
34	Low-temperature selective catalytic dehydrogenation of methylcyclohexane by surface protonics. RSC Advances, 2019, 9, 27743-27748.	1.7	21
35	Electric Field and Mobile Oxygen Promote Low-Temperature Oxidative Coupling of Methane over La _{1–<i>x</i>} Ca _{<i>x</i>} AlO _{3â~î´} Perovskite Catalysts. ACS Omega, 2019, 4, 10438-10443.	1.6	25
36	Promoting Discarded Packing Waste into Value-Added 2D Porous Carbon Flakes for Multifunctional Applications. ACS Sustainable Chemistry and Engineering, 2019, , .	3.2	0

#	Article	IF	CITATIONS
37	Enhanced methane activation on diluted metal–metal ensembles under an electric field: breakthrough in alloy catalysis. Chemical Communications, 2019, 55, 6693-6695.	2.2	33
38	Effect of Ba addition to Ga-α-Al2O3 catalyst on structure and catalytic selectivity for dehydrogenation of ethane. Applied Catalysis A: General, 2019, 581, 23-30.	2.2	21
39	Electrochemical deposition of self-supported bifunctional copper oxide electrocatalyst for methanol oxidation and oxygen evolution reaction. Journal of Industrial and Engineering Chemistry, 2019, 76, 515-523.	2.9	57
40	Highly Efficient g ₃ N ₄ Nanorods with Dual Active Sites as an Electrocatalyst for the Oxygen Evolution Reaction. ChemCatChem, 2019, 11, 2870-2878.	1.8	29
41	Roomâ€Temperature Ultrafast Synthesis of NiCoâ€Layered Double Hydroxide as an Excellent Electrocatalyst for Water Oxidation. ChemistrySelect, 2019, 4, 2409-2415.	0.7	25
42	High-Loading Carbon Nanotubes on Polymer Nanofibers as Stand-Alone Anode Materials for Li-Ion Batteries. ACS Omega, 2019, 4, 4129-4137.	1.6	14
43	Mgâ€lon Inversion in MgO@MgOâ^'Al ₂ O ₃ Oxides: The Origin of Basic Sites. ChemSusChem, 2019, 12, 2810-2818.	3.6	11
44	Irreversible catalytic methylcyclohexane dehydrogenation by surface protonics at low temperature. RSC Advances, 2019, 9, 5918-5924.	1.7	44
45	Hierarchical free-standing networks of MnCo2S4 as efficient Electrocatalyst for oxygen evolution reaction. Journal of Industrial and Engineering Chemistry, 2019, 71, 452-459.	2.9	37
46	Diamineâ€Functionalization of a Metal–Organic Framework Adsorbent for Superb Carbon Dioxide Adsorption and Desorption Properties. ChemSusChem, 2018, 11, 1694-1707.	3.6	40
47	Radical-initiated oxidative conversion of methane to methanol over metallic iron and copper catalysts. Molecular Catalysis, 2018, 445, 232-239.	1.0	9
48	In Situ Observation of Carbon Dioxide Capture on Pseudo-Liquid Eutectic Mixture-Promoted Magnesium Oxide. ACS Applied Materials & Interfaces, 2018, 10, 2414-2422.	4.0	47
49	Mechanistic insight into the quantitative synthesis of acetic acid by direct conversion of CH4 and CO2: An experimental and theoretical approach. Applied Catalysis B: Environmental, 2018, 229, 237-248.	10.8	59
50	Facile and cost-effective growth of a highly efficient MgCo ₂ O ₄ electrocatalyst for methanol oxidation. Inorganic Chemistry Frontiers, 2018, 5, 1115-1120.	3.0	34
51	Sacrificial templating method for fabrication of MgO-Al2O3@C spheres and their application to CO2 capture. Materials Letters, 2018, 211, 304-307.	1.3	7
52	Electron transport shuttle mechanism <i>via</i> an Fe–N–C bond derived from a conjugated microporous polymer for a supercapacitor. Dalton Transactions, 2018, 47, 852-858.	1.6	30
53	Collective use of deep eutectic solvent for one-pot synthesis of ternary Sn/SnO2@C electrode for supercapacitor. Journal of Alloys and Compounds, 2018, 732, 694-704.	2.8	24
54	Yolk-shelled ZnCo2O4 microspheres: Surface properties and gas sensing application. Sensors and Actuators B: Chemical, 2018, 257, 906-915.	4.0	197

#	Article	IF	CITATIONS
55	Self-assembled Mn ₃ O ₄ nano-clusters over carbon nanotube threads with enhanced supercapacitor performance. New Journal of Chemistry, 2018, 42, 19608-19614.	1.4	29
56	A comprehensive investigation of the condensation of furanic platform molecules to C ₁₄ –C ₁₅ fuel precursors over sulfonic acid functionalized silica supports. Green Chemistry, 2018, 20, 5133-5146.	4.6	38
57	Dual Role of Deep Eutectic Solvent as a Solvent and Template for the Synthesis of Octahedral Cobalt Vanadate for an Oxygen Evolution Reaction. ACS Sustainable Chemistry and Engineering, 2018, 6, 16255-16266.	3.2	54
58	Stabilization of NaNO ₃ -Promoted Magnesium Oxide for High-Temperature CO ₂ Capture. Environmental Science & Technology, 2018, 52, 11952-11959.	4.6	7
59	Tailoring and exploring the basicity of magnesium oxide nanostructures in ionic liquids for Claisen-Schmidt condensation reaction. Energy, 2018, 160, 635-647.	4.5	24
60	Mesoporous magnesium oxide nanoparticles derived via complexation-combustion for enhanced performance in carbon dioxide capture. Journal of Colloid and Interface Science, 2017, 498, 55-63.	5.0	33
61	Predictive Guide for Collective CO ₂ Adsorption Properties of Mgâ^'Al Mixed Oxides. ChemSusChem, 2017, 10, 1701-1709.	3.6	11
62	Mesoporous Mn ₂ O ₃ /reduced graphene oxide (rGO) composite with enhanced electrochemical performance for Li-ion battery. Dalton Transactions, 2017, 46, 9777-9783.	1.6	19
63	Synergistic activating effect of promoter and oxidant in single step conversion of methane into methanol over a tailored polymer-Ag coordination complex. RSC Advances, 2017, 7, 24168-24176.	1.7	4
64	Growth of urchin-like ZnCo2O4 microspheres on nickel foam as a binder-free electrode for high-performance supercapacitor and methanol electro-oxidation. Electrochimica Acta, 2017, 246, 941-950.	2.6	99
65	Fineâ€Tuning of the Carbon Dioxide Capture Capability of Diamineâ€Grafted Metal–Organic Framework Adsorbents Through Amine Functionalization. ChemSusChem, 2017, 10, 541-550.	3.6	88
66	Enhanced Cyclic Stability and CO2 Capture Performance of MgO-Al2O3 Sorbent Decorated with Eutectic Mixture. Energy Procedia, 2017, 114, 2421-2428.	1.8	8
67	Enhanced Selectivity for CO ₂ Adsorption on Mesoporous Silica with Alkali Metal Halide Due to Electrostatic Field: A Molecular Simulation Approach. ACS Applied Materials & Interfaces, 2017, 9, 31683-31690.	4.0	14
68	Electrochemical growth of Co(OH) ₂ nanoflakes on Ni foam for methanol electro-oxidation. New Journal of Chemistry, 2017, 41, 9546-9553.	1.4	56
69	Free standing growth of MnCo ₂ O ₄ nanoflakes as an electrocatalyst for methanol electro-oxidation. New Journal of Chemistry, 2017, 41, 15058-15063.	1.4	34
70	Bi-functionality of mesostructured MnCo2O4 microspheres for supercapacitor and methanol electro-oxidation. Ceramics International, 2017, 43, 2670-2679.	2.3	48
71	Controlled oxidation state of Ti in MgO-TiO 2 composite for CO 2 capture. Chemical Engineering Journal, 2017, 308, 177-183.	6.6	49
72	H 2 TiO 3 composite adsorbent foam for efficient and continuous recovery of Li + from liquid resources. Colloids and Surfaces A: Physicochemical and Engineering Aspects, 2016, 504, 267-279.	2.3	79

#	Article	IF	CITATIONS
73	SBA-15 supported ionic liquid phase (SILP) with H ₂ PW ₁₂ O ₄₀ ^{â^²} for the hydrolytic catalysis of red macroalgal biomass to sugars. RSC Advances, 2016, 6, 33901-33909.	1.7	18
74	Mixed matrix nanofiber as a flow-through membrane adsorber for continuous Li+ recovery from seawater. Journal of Membrane Science, 2016, 510, 141-154.	4.1	79
75	Induced application of biological waste Escherichia coli functionalized with an amine-based polymer for CO ₂ capture. RSC Advances, 2016, 6, 77535-77544.	1.7	2
76	Hierarchical Mesoporous 3D Flower-like CuCo2O4/NF for High-Performance Electrochemical Energy Storage. Scientific Reports, 2016, 6, 31120.	1.6	125
77	Template-Free Synthesis and Characterization of Nickel Oxide Nanocrystal with High-Energy Facets in Deep Eutectic Solvent. Journal of Nanoscience and Nanotechnology, 2016, 16, 11009-11013.	0.9	10
78	Liquid-liquid extraction of lithium using lipophilic dibenzo-14-crown-4 ether carboxylic acid in hydrophobic room temperature ionic liquid. Hydrometallurgy, 2016, 164, 362-371.	1.8	48
79	Green solvent ionic liquids: structural directing pioneers for microwave-assisted synthesis of controlled MgO nanostructures. RSC Advances, 2016, 6, 31675-31686.	1.7	28
80	Adsorptive Li+ mining from liquid resources by H2TiO3: Equilibrium, kinetics, thermodynamics, and mechanisms. Journal of Industrial and Engineering Chemistry, 2016, 35, 347-356.	2.9	99
81	One-pot synthesis of 2,5-diformylfuran from fructose using a magnetic bi-functional catalyst. RSC Advances, 2016, 6, 25678-25688.	1.7	41
82	Density functional theory approach to CO ₂ adsorption on a spinel mineral: determination of binding coordination. RSC Advances, 2016, 6, 28607-28611.	1.7	8
83	Effect of anion type of imidazolium based polymer supported ionic liquids on the solvent free synthesis of cycloaddition of CO2 into epoxide. Catalysis Today, 2016, 265, 56-67.	2.2	87
84	Self-assembled hierarchical 3D – NiO microspheres with ultra-thin porous nanoflakes for lithium-ion batteries. Journal of Power Sources, 2016, 302, 13-21.	4.0	79
85	Synthesis and Characterization of AlCl ₃ Impregnated Molybdenum Oxide as Heterogeneous Nano-Catalyst for the Friedel-Crafts Acylation Reaction in Ambient Condition. Journal of Nanoscience and Nanotechnology, 2015, 15, 8243-8250.	0.9	10
86	Organic radical functionalized SBA-15 as a heterogeneous catalyst for facile oxidation of 5-hydroxymethylfurfural to 2,5-diformylfuran. Journal of Molecular Catalysis A, 2015, 404-405, 106-114.	4.8	27
87	Synthesis of a dual-templated MgO–Al2O3 adsorbent using block copolymer and ionic liquid for CO2 capture. Chemical Engineering Journal, 2015, 270, 411-417.	6.6	21
88	Exceptional CO ₂ working capacity in a heterodiamine-grafted metal–organic framework. Chemical Science, 2015, 6, 3697-3705.	3.7	127
89	Esterification of carboxylic acids with alkyl halides using imidazolium based dicationic ionic liquids containing bis-trifluoromethane sulfonimide anions at room temperature. RSC Advances, 2015, 5, 26197-26208.	1.7	28
90	Homodiamine-functionalized metal–organic frameworks with a MOF-74-type extended structure for superior selectivity of CO ₂ over N ₂ . Journal of Materials Chemistry A, 2015, 3, 19177-19185.	5.2	75

#	Article	IF	CITATIONS
91	Synthesis and characterization of multi-walled carbon nanotubes-supported dibenzo-14-crown-4 ether with proton ionizable carboxyl sidearm as Li+ adsorbents. Chemical Engineering Journal, 2015, 264, 89-98.	6.6	56
92	Liquid–liquid extraction of Li+using mixed ion carrier system at room temperature ionic liquid. Desalination and Water Treatment, 2015, 53, 2774-2781.	1.0	23
93	High Temperature Carbon Dioxide Capture on Nano-Structured MgO–Al ₂ O ₃ and CaO–Al ₂ O ₃ Adsorbents: An Experimental and Theoretical Study. Iournal of Nanoscience and Nanotechnology. 2014. 14. 8531-8538.	0.9	19
94	Blended ionic liquid systems for macroalgae pretreatment. Renewable Energy, 2014, 66, 596-604.	4.3	32
95	Activated carbon aerogel containing graphene as electrode material for supercapacitor. Materials Research Bulletin, 2014, 50, 240-245.	2.7	50
96	Elevated temperature CO2 capture on nano-structured MgO–Al2O3 aerogel: Effect of Mg/Al molar ratio. Chemical Engineering Journal, 2014, 242, 357-363.	6.6	87
97	Metal-free mild oxidation of 5-hydroxymethylfurfural to 2,5-diformylfuran. Korean Journal of Chemical Engineering, 2014, 31, 1362-1367.	1.2	27
98	Recyclable composite nanofiber adsorbent for Li+ recovery from seawater desalination retentate. Chemical Engineering Journal, 2014, 254, 73-81.	6.6	150
99	Hydrogen production by steam reforming of ethanol over mesoporous Ni–Al2O3–ZrO2 aerogel catalyst. International Journal of Hydrogen Energy, 2013, 38, 15119-15127.	3.8	31
100	Hydrogen production by steam reforming of ethanol over mesoporous Ni–Al2O3–ZrO2 xerogel catalysts: Effect of nickel content. International Journal of Hydrogen Energy, 2013, 38, 8285-8292.	3.8	40
101	Hydrogen production by steam reforming of ethanol over mesoporous Ni–Al2O3–ZrO2 xerogel catalysts: Effect of Zr/Al molar ratio. International Journal of Hydrogen Energy, 2013, 38, 1376-1383.	3.8	38
102	Hydrogen production by steam reforming of liquefied natural gas (LNG) over trimethylbenzene-assisted ordered mesoporous nickel–alumina catalyst. International Journal of Hydrogen Energy, 2013, 38, 8751-8758.	3.8	27
103	Methanation of carbon dioxide over mesoporous Ni–Fe–Al2O3 catalysts prepared by a coprecipitation method: Effect of precipitation agent. Journal of Industrial and Engineering Chemistry, 2013, 19, 2016-2021.	2.9	82
104	Hydrogen production by steam reforming of liquefied natural gas (LNG) over mesoporous nickel–aluminaÂxerogel catalysts prepared by a single-step carbon-templating sol–gel method. International Journal of Hydrogen Energy, 2012, 37, 11208-11217.	3.8	18
105	Hydrogen production by steam reforming of liquefied natural gas (LNG) over ordered mesoporous nickel–alumina catalyst. International Journal of Hydrogen Energy, 2012, 37, 17967-17977.	3.8	43
106	Hydrogen production by steam reforming of liquefied natural gas (LNG) over mesoporous Ni-Al2O3 aerogel catalyst prepared by a single-step epoxide-driven sol-gel method. International Journal of Hydrogen Energy, 2012, 37, 1436-1443.	3.8	27
107	Hydrogenation of succinic acid to γ-butyrolactone (GBL) over palladium catalyst supported on alumina xerogel: Effect of acid density of the catalyst. Journal of Industrial and Engineering Chemistry, 2011, 17, 316-320.	2.9	50
108	Preparation and performance of cobalt-doped carbon aerogel for supercapacitor. Korean Journal of Chemical Engineering, 2011, 28, 492-496.	1.2	12

#	Article	IF	CITATIONS
109	Nano-sized metal-doped carbon aerogel for pseudo-capacitive supercapacitor. Current Applied Physics, 2011, 11, 631-635.	1.1	29
110	Hydrogen production by steam reforming of simulated liquefied natural gas (LNG) over mesoporous nickel–M–alumina (M=Ni, Ce, La, Y, Cs, Fe, Co, and Mg) aerogel catalysts. International Journal of Hydrogen Energy, 2011, 36, 3505-3514.	3.8	21
111	Hydrogen production by steam reforming of liquefied natural gas (LNG) over mesoporous Ni–La–Al2O3 aerogel catalysts: Effect of La content. International Journal of Hydrogen Energy, 2011, 36, 8307-8315.	3.8	62
112	Methane production from carbon monoxide and hydrogen over nickel–alumina xerogel catalyst: Effect of nickel content. Journal of Industrial and Engineering Chemistry, 2011, 17, 154-157.	2.9	90
113	Pd catalyst supported on SiO2–Al2O3 xerogel for hydrocracking of paraffin wax to middle distillate. Journal of Industrial and Engineering Chemistry, 2011, 17, 310-315.	2.9	21
114	Acidity and acid catalysis of polyatom-substituted H n PW11M1O40 (M=V, Nb, Ta, and W) Keggin heteropolyacid catalysts. Korean Journal of Chemical Engineering, 2010, 27, 465-468.	1.2	5
115	Production of middle distillate through hydrocracking of paraffin wax over Pd0.15Cs x H2.7â^'x PW12O40 catalysts: Effect of cesium content and surface acidity. Korean Journal of Chemical Engineering, 2010, 27, 807-811.	1.2	5
116	Hydrogenation of Succinic Acid to γ-Butyrolactone over Palladium Catalyst Supported on Mesoporous Alumina Xerogel. Catalysis Letters, 2010, 138, 28-33.	1.4	27
117	Mesoporous Nickel–Alumina Catalysts for Hydrogen Production by Steam Reforming of Liquefied Natural Gas (LNG). Catalysis Surveys From Asia, 2010, 14, 1-10.	1.0	10
118	Support Modification of Supported Nickel Catalysts for Hydrogen Production by Auto-thermal Reforming of Ethanol. Catalysis Surveys From Asia, 2010, 14, 55-63.	1.0	10
119	Deactivation behaviors of hybrid Fischer–Tropsch catalysts in the production of middle distillate from synthesis gas in a dual-bed reactor. Research on Chemical Intermediates, 2010, 36, 685-692.	1.3	4
120	Effect of calcination temperature of mesoporous nickel–alumina catalysts on their catalytic performance in hydrogen production by steam reforming of liquefied natural gas (LNG). Journal of Industrial and Engineering Chemistry, 2010, 16, 795-799.	2.9	31
121	Production of middle distillate through hydrocracking of paraffin wax over Pd/SiO2–Al2O3 catalysts. Journal of Industrial and Engineering Chemistry, 2010, 16, 790-794.	2.9	18
122	Hydrogen production by auto-thermal reforming of ethanol over nickel catalyst supported on metal oxide-stabilized zirconia. International Journal of Hydrogen Energy, 2010, 35, 3490-3498.	3.8	28
123	Hydrogen production by steam reforming of liquefied natural gas (LNG) over mesoporous nickel–alumina aerogel catalyst. International Journal of Hydrogen Energy, 2010, 35, 6738-6746.	3.8	37
124	Effect of Ni/Al atomic ratio of mesoporous Ni–Al2O3 aerogel catalysts on their catalytic activity for hydrogen production by steam reforming of liquefied natural gas (LNG). International Journal of Hydrogen Energy, 2010, 35, 12174-12181.	3.8	26
125	Hydrogen production by auto-thermal reforming of ethanol over nickel catalysts supported on metal oxides: Effect of support acidity. Applied Catalysis B: Environmental, 2010, 98, 57-64.	10.8	60
126	Hydrogen Production by Steam Reforming of Liquefied Natural Gas over Mesoporous Ni-Al2O3 Catalysts Prepared by a Co-Precipitation Method: Effect of Ni/Al Atomic Ratio. Catalysis Letters, 2009, 130, 410-416.	1.4	20

#	Article	IF	Citations
127	Effect of Calcination Temperature on the Catalytic Performance of Î ³ -Bi2MoO6 in the Oxidative Dehydrogenation of n-Butene to 1,3-Butadiene. Catalysis Letters, 2009, 131, 401-405.	1.4	14

Redox Properties and Catalytic Oxidation Activities of Polyatom-Substituted H n PW11M1O40 ($M\hat{A}=\hat{A}V$, Nb,) Tj ETQq0 0 0 rgBT /Overload ($M\hat{A}=\hat{A}V$, Nb,) Tj ETQq0 0 0 rgBT /Overload ($M\hat{A}=\hat{A}V$, Nb,) Tj ETQq0 0 0 rgBT /Overload ($M\hat{A}=\hat{A}V$, Nb,) Tj ETQq0 0 0 rgBT /Overload ($M\hat{A}=\hat{A}V$, Nb,) Tj ETQq0 0 0 rgBT /Overload ($M\hat{A}=\hat{A}V$, Nb,) Tj ETQq0 0 0 rgBT /Overload ($M\hat{A}=\hat{A}V$, Nb,) Tj ETQq0 0 0 rgBT /Overload ($M\hat{A}=\hat{A}V$, Nb,) Tj ETQq0 0 0 rgBT /Overload ($M\hat{A}=\hat{A}V$, Nb,) Tj ETQq0 0 0 rgBT /Overload ($M\hat{A}=\hat{A}V$, Nb,) Tj ETQq0 0 0 rgBT /Overload ($M\hat{A}=\hat{A}V$, Nb,) Tj ETQq0 0 0 rgBT /Overload ($M\hat{A}=\hat{A}V$, Nb,) Tj ETQq0 0 0 rgBT /Overload ($M\hat{A}=\hat{A}V$, Nb,) Tj ETQq0 0 0 rgBT /Overload ($M\hat{A}=\hat{A}V$, Nb,) Tj ETQq0 0 0 rgBT /Overload ($M\hat{A}=\hat{A}V$) ($M\hat{A}=\hat{A}V$, Nb,) Tj ETQq0 0 0 rgBT /Overload ($M\hat{A}=\hat{A}V$) ($M\hat$

129	Preparation and Oxidation Catalysis of H5PMo10V2O40 Catalyst Immobilized on Nitrogen-Containing Spherical Carbon. Catalysis Letters, 2009, 132, 377-382.	1.4	10
130	Hydrogen Production by Steam Reforming of Liquefied Natural Gas Over Mesoporous Ni-Al2O3 Composite Catalyst Prepared by a Single-step Non-ionic Surfactant-templating Method. Catalysis Letters, 2009, 132, 395-401.	1.4	17
131	Production of Middle Distillate Through Hydrocracking of Paraffin Wax Over NiMo/SiO2-Al2O3 Catalysts: Effect of Solvent in the Preparation of SiO2-Al2O3 by a Sol–Gel Method. Catalysis Letters, 2009, 132, 410-416.	1.4	9
132	Production of Middle Distillate from Synthesis Gas in a Dual-bed Reactor Through Hydrocracking of Wax Over Mesoporous Pd-Al2O3 Composite Catalyst. Catalysis Letters, 2009, 130, 192-197.	1.4	15
133	Direct Synthesis of Hydrogen Peroxide from Hydrogen and Oxygen Over Palladium Catalysts Supported on SO3H-Functionalized SiO2 and TiO2. Catalysis Letters, 2009, 130, 604-607.	1.4	20
134	Hydrogen production by steam reforming of liquefied natural gas (LNG) over nickel catalyst supported on mesoporous alumina prepared by a non-ionic surfactant-templating method. International Journal of Hydrogen Energy, 2009, 34, 1809-1817.	3.8	49
135	Hydrogen production by steam reforming of liquefied natural gas (LNG) over Ni/Al2O3–ZrO2 xerogel catalysts: Effect of calcination temperature of Al2O3–ZrO2 xerogel supports. International Journal of Hydrogen Energy, 2009, 34, 3755-3763.	3.8	62
136	Effect of preparation method of mesoporous Ni–Al2O3 catalysts on their catalytic activity for hydrogen production by steam reforming of liquefied natural gas (LNG). International Journal of Hydrogen Energy, 2009, 34, 5409-5416.	3.8	31
137	Hydrogen production by auto-thermal reforming of ethanol over nickel catalyst supported on mesoporous yttria-stabilized zirconia. International Journal of Hydrogen Energy, 2009, 34, 5390-5397.	3.8	29
138	Hydrogen production by steam reforming of liquefied natural gas (LNG) over Ni–Al2O3 catalysts prepared by a sequential precipitation method: Effect of precipitation agent. International Journal of Hydrogen Energy, 2009, 34, 8053-8060.	3.8	14
139	Hydrogen production by steam reforming of liquefied natural gas (LNG) over nickel catalysts supported on cationic surfactant-templated mesoporous aluminas. Journal of Power Sources, 2009, 186, 178-184.	4.0	24
140	Hydrogen production by auto-thermal reforming of ethanol over Ni-Ti-Zr metal oxide catalysts. Renewable Energy, 2009, 34, 731-735.	4.3	14
141	Hydrogen production by auto-thermal reforming of ethanol over Ni catalyst supported on ZrO2 prepared by a sol–gel method: Effect of H2O/P123 mass ratio in the preparation of ZrO2. Catalysis Today, 2009, 146, 57-62.	2.2	24
142	Hydrogen production by steam reforming of liquefied natural gas (LNG) over mesoporous nickel–alumina composite catalyst prepared by an anionic surfactant-templating method. Catalysis Today, 2009, 146, 44-49.	2.2	28
143	Effect of calcination temperature of alumina supports on the wax hydrocracking performance of Pd-loaded mesoporous alumina xerogel catalysts for the production of middle distillate. Chemical Engineering Journal, 2009, 146, 307-314.	6.6	32
144	Epoxidation of Propylene with Hydrogen Peroxide Over TS-1 Catalyst Synthesized in the Presence of Polystyrene. Catalysis Letters, 2008, 122, 349-353.	1.4	20

9

#	Article	IF	CITATIONS
145	Effect of Al2O3-ZrO2 xerogel support on hydrogen production by steam reforming of LNG over Ni/Al2O3-ZrO2 catalyst. Korean Journal of Chemical Engineering, 2008, 25, 41-45.	1.2	76
146	Hydrogen production by steam reforming of LNG over Ni/Al2O3-ZrO2 catalysts: Effect of ZrO2 and preparation method of Al2O3-ZrO2. Korean Journal of Chemical Engineering, 2008, 25, 95-98.	1.2	37
147	Effect of support on hydrogen production by auto-thermal reforming of ethanol over supported nickel catalysts. Korean Journal of Chemical Engineering, 2008, 25, 236-238.	1.2	46
148	Production of middle distillate in a dual-bed reactor from synthesis gas through wax cracking: Effect of acid property of Pd-loaded solid acid catalysts on the wax conversion and middle distillate selectivity. Applied Catalysis B: Environmental, 2008, 83, 195-201.	10.8	35
149	Preparation of Ni/Al2O3–ZrO2 catalysts and their application to hydrogen production by steam reforming of LNG: Effect of ZrO2 content grafted on Al2O3. Catalysis Today, 2008, 138, 130-134.	2.2	27
150	Hydrogen production by steam reforming of liquefied natural gas (LNG) over mesoporous nickel–alumina xerogel catalysts: Effect of nickel content. Chemical Engineering Journal, 2008, 141, 298-304.	6.6	51
151	Hydrogen production by auto-thermal reforming of ethanol over nickel catalysts supported on Ce-modified mesoporous zirconia: Effect of Ce/Zr molar ratio. International Journal of Hydrogen Energy, 2008, 33, 5052-5059.	3.8	58
152	Effect of calcination temperature of mesoporous alumina xerogel (AX) supports on hydrogen production by steam reforming of liquefied natural gas (LNG) over Ni/AX catalysts. International Journal of Hydrogen Energy, 2008, 33, 7427-7434.	3.8	36
153	Hydrogen production by auto-thermal reforming of ethanol over Ni catalysts supported on ZrO2: Effect of preparation method of ZrO2 support. International Journal of Hydrogen Energy, 2008, 33, 7457-7463.	3.8	30
154	Role and effect of molybdenum on the performance of Ni-Mo/γ-Al2O3 catalysts in the hydrogen production by auto-thermal reforming of ethanol. Journal of Molecular Catalysis A, 2007, 261, 276-281.	4.8	80
155	Hydrogen production by steam reforming of LNG over Ni/Al2O3–ZrO2 catalysts: Effect of Al2O3–ZrO2 supports prepared by a grafting method. Journal of Molecular Catalysis A, 2007, 268, 9-14.	4.8	52
156	Effect of SiO2-ZrO2 supports prepared by a grafting method on hydrogen production by steam reforming of liquefied natural gas over Ni/SiO2-ZrO2 catalysts. Journal of Power Sources, 2007, 168, 251-257.	4.0	20
157	Hydrogen production by steam reforming of liquefied natural gas over a nickel catalyst supported on mesoporous alumina xerogel. Journal of Power Sources, 2007, 173, 943-949.	4.0	32
158	Hydrogen production by auto-thermal reforming of ethanol over Ni/γ-Al2O3 catalysts: Effect of second metal addition. Journal of Power Sources, 2006, 162, 1270-1274.	4.0	50